

Long range dynamical coupling between magnetic adatoms mediated by a 2D topological insulator

M. Costa,¹ M. Buongiorno Nardelli,^{2,3} A. Fazio,¹ and A. T. Costa^{4,1,5}

¹*Brazilian Nanotechnology National Laboratory (LNNano), CNPEM, 13083-970 Campinas, Brazil.*

²*Department of Physics and Department of Chemistry, University of North Texas, Denton TX, USA.*

³*Center for Materials Genomics, Duke University, Durham, NC 27708, USA.*

⁴*Instituto de Telecomunicações, Physics of Information and Quantum Technologies Group, Lisbon, Portugal.*

⁵*Instituto de Física, Universidade Federal Fluminense, 24210-346 Niterói, RJ, Brazil.**

We study the spin excitation spectra and the dynamical exchange coupling between iron adatoms on a Bi bilayer nanoribbon. We show that the topological character of the edge states is preserved in the presence of the magnetic adatoms. Nevertheless, they couple significantly to the edge spin currents, as witnessed by the large and long-ranged dynamical coupling we obtain in our calculations. The large effective magnetocrystalline anisotropy of the magnetic adatoms combined with the transport properties of the topologically protected edge states make this system a strong candidate for implementation of spintronics devices and quantum information and/or computation protocols.

INTRODUCTION

Topological quantum matter has been recognized as a fundamental concept in physics as well as a huge promise for future quantum technologies [1–3]. The peculiar properties of topologically protected edge states (TPES) have been hailed as a “Holy Grail” for quantum information processing [4]. Heterostructures combining topological insulators and other “non-trivial” matter, such as superconductors, hold promises for even more intriguing states, such as Majorana fermions [5, 6].

Magnetic systems of nanoscopic dimensions have also been considered as candidates for implementation of quantum technologies. Proposals range from controlling electronic spins in quantum dots [7] to manipulate individual atomic magnetizations on surfaces [8].

The idea of depositing magnetic atoms on two-dimensional topological insulators has particularly enticing aspects. From the fundamental point of view, it is intriguing to enquire about the strength and nature of the coupling between magnetic units and the topologically protected edge states. From the technological side, functionalization with magnetic adatoms may be an efficient route to tap into the attractive properties of TPES [9, 10]. As an added bonus, the high spin-orbit coupling strength necessary to produce topologically non-trivial states may also endow magnetic adatoms with magnetocrystalline anisotropy large enough to stabilize the magnetization direction against quantum and thermal fluctuations. Two general questions immediately come to mind: How does the presence of magnetic impurities affect topological protection, considering it breaks time-reversal symmetry? and How does the topological nature of the substrate affect the properties of the magnetic unities and its interactions? To try and answer these questions is the main motivation of this work.

The study of spin excitations provide a prolific source of information on the properties of magnetic systems.

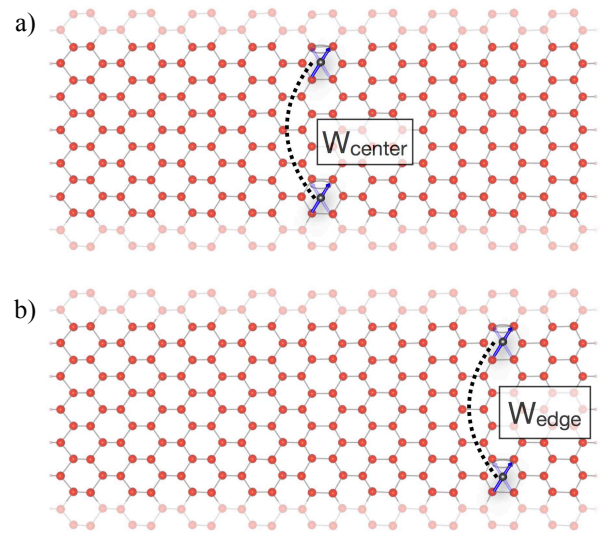


FIG. 1. Schematic picture of the two magnetic impurities configuration, at the (a) center and (b) edge of the nanoribbon. The nanoribbon is wide enough to minimize the presence of the topological edge states in its middle region (center). There is a remarkably difference in their interaction (W) at the two considered positions.

It can reveal the nature and magnitudes of individual contributions to the system’s energy (such as exchange, anisotropy, etc.) as well as relaxation and absorption properties. Spin excitations in individual magnetic adatoms have been probed experimentally with inelastic tunneling spectroscopy [11, 12], revealing the peculiarities of the magnetization dynamics at the atomic scale. Theoretical knowledge of the spin excitation spectra of such systems has been instrumental in the design and interpretation of those experiments.

In this letter we investigate theoretically, employing a combination of combination of *ab initio* DFT calculations, realistic tight-binding models and many-body techniques, the ground state and magnetic excitations of Fe

adatoms on a Bi bilayer nanoribbon. The Bi bilayer is a promising TI with a 500 meV gap [13–18], which is originated from the large Bi SOC. We consider isolated adatoms and pairs of adatoms deposited on an otherwise pristine ribbon. The ribbon’s width is large enough to guarantee the existence of topologically protected edge states [16]. We investigate the indirect exchange coupling (sometimes dubbed RKKY coupling) through the substrate and show that, for the smallest distances considered, it is essentially zero. We focus our attention on the dynamical coupling that appears as a result of the exchange of pure spin currents between the out-of-equilibrium magnetizations of the Fe adatoms. We show that it is very long ranged as a result of the peculiar properties of the TPES.

METHODOLOGY

We use a multi-orbital tight-binding Hamiltonian to describe the electronic structure of the decorated nanoribbon. The full hamiltonian can be written as the sum of band energy H_0 , effective intra-atomic Coulomb repulsion H_I and the atomic spin-orbit coupling H_{SOC} . The band energy H_0 is given by,

$$H_0 = \sum_{l'} \sum_{\mu\nu} \sum_{\sigma} T_{ll'}^{\mu\nu} c_{l\mu\sigma}^\dagger c_{l'\nu\sigma}. \quad (1)$$

where $T_{ll'}^{\mu\nu}$ is the hopping matrix, σ is a spin index, l, l' are atomic site indices and μ, ν are atomic orbital indices. The hopping matrix is obtained directly from a DFT calculation using the pseudo atomic orbital projection method [19–23]. The method consists in projecting the Hilbert space spanned by the plane waves onto a compact subspace composed of the pseudo atomic orbitals (PAO). These PAOs functions are naturally built into the pseudo potential used in the DFT calculation.

The atomic spin-orbit coupling (SOC) is introduced in a effective approximation,

$$H_{SOC} = \sum_l \sum_{\mu\nu} \sum_{\sigma\sigma'} \xi_l^{\mu\nu} \langle l\mu\sigma | \vec{L} \cdot \vec{S} | l\nu\sigma' \rangle c_{l\mu\sigma}^\dagger c_{l\nu\sigma'} \quad (2)$$

where \vec{L} and \vec{S} are the orbital and spin angular momentum operators, respectively. The SOC strength is given by $\xi_l^{\mu\nu}$ and is also obtained from the DFT calculations.

The magnetism of the Fe adatoms is driven by the effective intra-atomic Coulomb repulsion

$$H_I = \sum_l \sum_{\mu\nu\mu'\nu'} \sum_{\sigma\sigma'} U_l^{\mu\nu\mu'\nu'} c_{l\mu\sigma}^\dagger c_{l\nu\sigma'}^\dagger c_{l\nu'\sigma'} c_{l\mu'\sigma}. \quad (3)$$

The spin-polarized ground state is obtained from a self-consistent mean-field treatment of the effective Coulomb repulsion term, Eq. (3). Both magnitude and direction of the magnetization at each adatom are found as solutions of the self-consistency equations. After a solution

is found, a calculation of the spin excitation spectrum reveals whether it is a stable or unstable solution. In the latter case, we search for a new solution, usually starting from a high symmetry configuration. The comparison between the band structures from the DFT and the multi-orbital tight-binding Hamiltonian are shown in the supplemental material [24] along with the procedure to obtain the SOC strength $\xi_l^{\mu\nu}$.

The spin excitation spectrum is obtained from the spin susceptibility matrix $\chi_{\mu\nu}^{ab}(l, l')$, where $a, b \in \{+, -, \uparrow, \downarrow\}$ [25, 26]. For instance, if the equilibrium magnetization lies along the z direction, the transverse spin excitation spectrum is given by $\chi_{\mu\nu}^{+-}(l, l')$. For a general magnetization vector, however, a more complicated combination of the matrix elements χ^{ab} will result from applying to it the appropriate rotation transformations.

The spin susceptibility matrix elements are the propagators

$$\chi_{\mu\nu}^{ab}(l, l' | t - t') = -i\theta(t - t') \langle\langle S_{l\mu}^a(t), S_{l'\nu}^b(t') \rangle\rangle. \quad (4)$$

Due to the interaction term Eq. 3, the equations of motion for χ^{ab} are coupled to higher order propagators, in an infinite chain. We employ a decoupling scheme that is frequently dubbed “time dependent Hartree-Fock”. It is equivalent to the summation of the infinite series for the electron-hole pair ladder diagrams, and leads to the collective spin excitation modes identified with the poles of χ^{ab} . In translation-invariant systems those modes are the spin waves; when the magnetic entities are confined in space the spin excitation modes are akin to normal modes of coupled oscillators. In the presence of spin-orbit coupling the transverse spin excitations are coupled to longitudinal excitations and charge excitations. This is reflected in the fact that the equations of motion for all the elements of χ^{ab} have to be solved simultaneously. The solution has been presented in detail in reference [25]. The physical consequences of this dynamical spin-charge coupling have been little explored hitherto, but we intend to divulge the results of our investigations on this matter in future publications.

When considered as a matrix in site indices, the transverse susceptibility $\chi_{ll'}^{+-}$ yields two very relevant sets of informations: the imaginary part of its diagonal elements represent the local (atomic site) projection of the magnon spectral density, or the local magnon density of states. From it we can extract the magnon’s energies and lifetimes. The off-diagonal terms represent non-local response functions, and inform about the excitation of a magnon at site l due to the application of a transverse field at site l' . It is important to notice that this “dynamical coupling” may exist even when $|\vec{R}_l - \vec{R}_{l'}|$ is so large that the (RKKY) indirect exchange coupling is utterly negligible [27, 28]. Its physical origin is the spin current shed by the spin excitation at l' , which flows through the supporting medium and reaches site l , thus imparting a

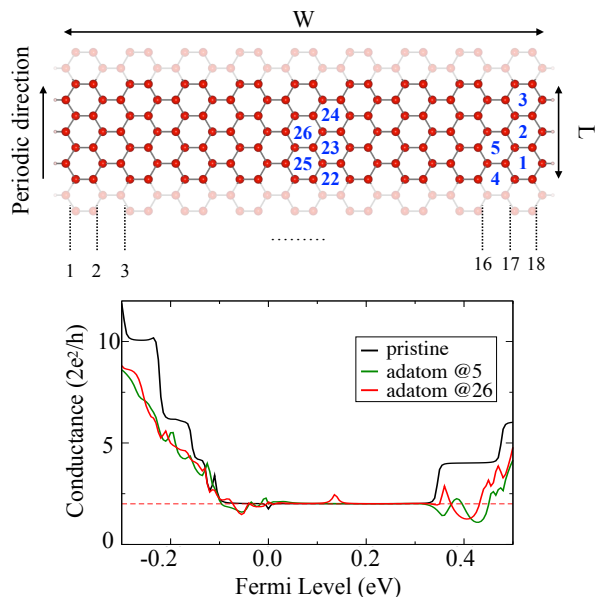


FIG. 2. Top panel shows the Bi zigzag nanoribbon structure with 18 zigzag units and a width (W) of 65 Å. The length (L) is equal to 13.05 Å along the periodic direction. The adsorption sites are labeled, from right to left, as shown by the blue numbers. In bottom panel the pristine, adatom @26 and adatom @5 conductance is shown.

torque on the magnetization there. We chose to represent the intensity of the dynamical coupling between sites l and l' as the amplitude of the magnetization precession at site l due to a transverse, circularly polarized magnetic field applied at site l' .

RESULTS AND DISCUSSION

We begin by showing that the topologically protected edge states (TPES) of the Bi bilayer nanoribbon are negligibly perturbed by the presence of the adatoms. In figure 2, bottom panel, we compare the conductance of the pristine nanoribbon with that of the ribbons decorated with a single Fe adatom. It is clear that the conductance of the TPES is preserved over most of the bulk gap for all adatoms positions considered. The behavior of the edge spin currents as a function of energy are modified by the adatoms, but their overall order of magnitude is preserved.

The magnetic moments of the adatoms have been determined selfconsistently, both in size and direction. For a single adatom at the center of the ribbon the magnetic moment is mostly perpendicular to the plane of the ribbon, with a small in-plane component perpendicular to the ribbon's length. For the adatom close to the edge the magnetic moment becomes almost parallel to the plane of the ribbon.

The spectral densities for transverse spin excitations for single adatoms at different positions across the rib-

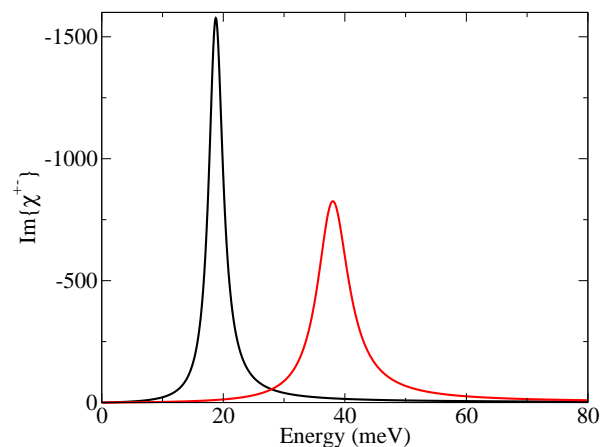


FIG. 3. Spectral densities for transverse spin excitations of single adatoms adsorbed to the Bi bilayer nanoribbon at two distinct sites: close to one edge (@5, black line) and at the center of the ribbon (@26, red line).

bon are shown in figure 3. From those spectral densities we can extract an effective magnetocrystalline anisotropy energy (eMAE) [29] and the damping rate (or equivalently, the lifetime) of the transverse spin excitations. For the adatom at the center of the ribbon the eMAE is 38 meV, which corresponds to a precession frequency of approximately 9.2 THz. The eMAE for the adatom close to the edge is 19 meV ($\nu_0 \approx 4.6$ THz). Although the nominal excitation lifetime for the adatom close to the edge is larger, the quality factors for both positions are very similar ($Q = 12$ for the center and $Q = 13$ close to the edge). Notice that the MAE we obtained is completely due to the huge spin-orbit coupling strength of Bi ($\xi_{\text{Bi}} = 1.475$ eV), since the tiny SOC strength of Fe ($\xi_{\text{Fe}} = 0.08$ eV) was not even included in our calculations.

It is interesting to notice that transverse spin excitations of adatoms on insulating surfaces usually have much longer lifetimes than those we obtained. [11] The large damping is certainly due to the huge SOC strength of Bi. However, we speculate that the spin angular momentum associated with the spin excitation has first to penetrate into the Bi substrate in order to be then transferred to the orbital degrees of freedom and ultimately be dissipated by the lattice vibrations. The fact that spin currents can easily flow into a non-magnetic insulating substrate may seem somewhat counterintuitive, but in what follows we will show that this is indeed the case.

We now turn to the spin excitations of pairs of Fe adatoms. We are mainly interested in the behavior of the transverse spin excitation spectra as the distance between the adatoms is varied. As we will show, for almost all distances considered there is no Heisenberg-like indirect exchange coupling between the adatoms. However, a large dynamical coupling appears as soon as the magnetic moments are driven away from equilibrium in a time-dependent manner. We choose as a measure of

the dynamical coupling the norm of the transverse magnetization induced at adatom 2 due to a transverse field applied to adatom 1. This is proportional to the non-local susceptibility χ_{12}^{+-} , as detailed in reference [30]. In figure 4 we show the dynamical coupling as a function of energy for various distances between the adatoms. In each case the adatoms are placed in the nanoribbon on the same position relative to the edge. In the top panel the adatoms are close to the edge and in the bottom panel they are adsorbed at the center of the nanoribbon. It is clear that the dynamical coupling decreases abruptly as a function of distance for the adatoms at the central sites, but only slightly for the adatoms close to the edge. This is an indication that the topologically protected edge states have an essential role in mediating the dynamical coupling between the adatoms. To highlight the importance of the topologically protected edge states as mediators of the dynamical coupling, we reduced by hand the spin-orbit coupling in Bi to 0.8 eV and repeated the calculations. For this value of the SOC strength the Bi bilayer nanoribbon is a non-topological insulator and there are no TPES. In figure 5 we compare the behavior of the dynamical coupling as a function of the distance between the adatoms in the two cases, “real” Bi, and Bi with an artificially reduced SOC strength. For both the adatom close to the edge and at the center of the ribbon, the dynamical coupling decays exponentially with the distance for the reduced SOC case. This is markedly different from the behavior of the real system. There, only a slight, polynomial decay is observed when the adatoms are close to the edge. For the adatoms at the center the decay is faster, although definitely not exponential, and the dynamic coupling reaches a plateau for distances larger than about 8 nm. We interpret these results as evidence that the topologically protected edge states play a crucial role in carrying the spin currents responsible for the dynamical coupling between the adatoms’ magnetic moments. There is a curious interplay here, because the strong SOC of Bi would be expected to scramble spin information rapidly for spin currents flowing through a non-topological material made of Bi. In the language commonly used in the spin transport community, Bi materials would be considered almost ideal spin sinks. The existence of topologically protected edge states, however, render Bi bilayer an almost ideal spin current conduit, enabling spin information to be transported through large distances with very small losses.

CONCLUDING REMARKS

We used a combination of DFT calculations and multi-orbital tight-binding hamiltonians to study the collective spin excitations of magnetic adatoms on a two-dimensional topological insulator. We have shown that the large spin-orbit coupling in Bi induces unusually large

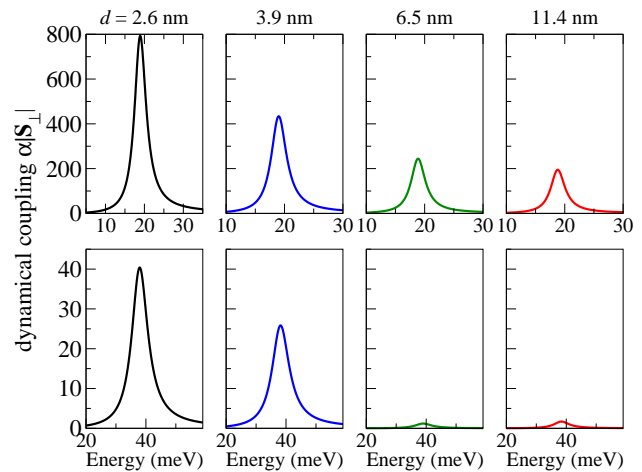


FIG. 4. Dynamical coupling as a function of excitation frequency for selected inter-adatoms distances. The top panel corresponds to the adatoms adsorbed close to one of the ribbon’s edges (@5). The bottom panel corresponds to the adatoms adsorbed to the center of the ribbon (@26).

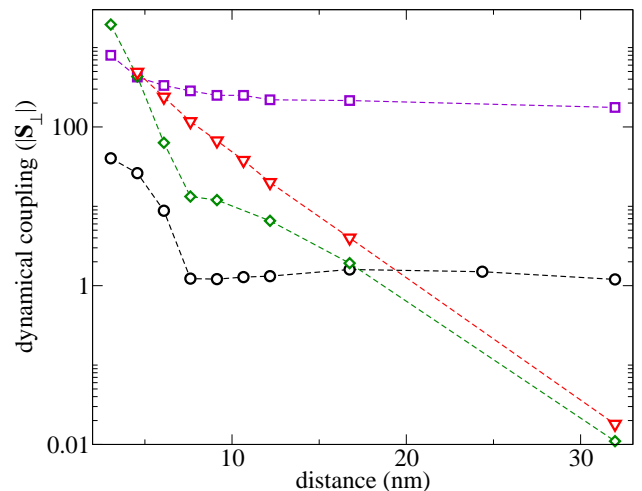


FIG. 5. Dynamical coupling as a function of the inter-adatom distance at resonance. Circles and squares correspond to the adatoms adsorbed to the center and close to the edge of the ribbon, respectively. The values depicted using triangles and diamonds were obtained by artificially suppressing the strength of spin-orbit coupling in Bi to 0.8 eV, such that no topologically protected edge states exist in the nanoribbon.

effective magnetocrystalline anisotropy energies in the Fe adatoms, which result in spin excitation frequencies within the terahertz range. Most importantly, we have shown that the topologically protected edge states of the Bi bilayer nanoribbon mediate a long range dynamical coupling between the adatoms’ magnetic moments. This coupling is a consequence of the almost unperturbed flow of spin currents between two distant adatoms. We believe these findings indicate an effective way to couple exter-

nal probes to topologically protected edge states. They also highlight the unusual and potentially very useful spin transport properties of two-dimensional topological insulators. Moreover, the findings we reported show unequivocally that there is much to be learned by building hybrid structures from topological insulators and magnetic materials.

ACKNOWLEDGEMENT

This work was supported by the Brazilian agencies FAPESP, through the Grant TEMÁTICO (2017/02327-2), and CNPq. We would like to acknowledge computing time provided by Laboratório de Computação Científica Avancada (Universidade de São Paulo). MBN acknowledges support by DOD-ONR (N00014-13-1-0635, N00014-11-1-0136, N00014-15-1-2863), the High Performance Computing Center at the University of North Texas, and the Texas Advanced Computing Center at the University of Texas, Austin. ATC wishes to acknowledge partial financial support from Fundação para a Ciência e a Tecnologia (Portugal), namely through programmes PTDC/POPH/POCH and projects UID/EEA/50008/2013, IT/QuNet, partially funded by EU FEDER, from the QuantERA project TheBlinQC, and from the JTF project NQuN (ID 60478), and FAPESP (Brazil). ATC is also indebted to R. Bechara Muniz and F. S. M. Guimarães for enlightening discussions.

* antoniocosta@id.uff.br

- [1] F. D. M. Haldane, *Rev. Mod. Phys.* **89**, 040502 (2017).
- [2] M. Z. Hasan and C. L. Kane, *Rev. Mod. Phys.* **82**, 3045 (2010).
- [3] X.-L. Qi and S.-C. Zhang, *Rev. Mod. Phys.* **83**, 1057 (2011).
- [4] G. J. Ferreira and D. Loss, *Phys. Rev. Lett.* **111**, 106802 (2013).
- [5] L. Fu and C. L. Kane, *Phys. Rev. Lett.* **100**, 096407 (2008).
- [6] C. Beenakker, *Annual Review of Condensed Matter Physics* **4**, 119 (2013), <https://doi.org/10.1146/annurev-conmatphys-030212-184337>.
- [7] P. Pfeffer, F. Hartmann, I. Neri, A. Schade, M. Emerling, M. Kamp, L. Gammaioni, S. Hfling, and L. Worschech, *Nanotechnology* **27**, 215201 (2016).
- [8] A. A. Khajetoorians, J. Wiebe, B. Chilian, and R. Wiesendanger, *Science* **332**, 1062 (2011).
- [9] J. Honolka, A. A. Khajetoorians, V. Sessi, T. O. Wehling, S. Stepanow, J.-L. Mi, B. B. Iversen, T. Schlenk, J. Wiebe, N. B. Brookes, A. I. Lichtenstein, P. Hofmann, K. Kern, and R. Wiesendanger, *Phys. Rev. Lett.* **108**, 256811 (2012).
- [10] J. Kim and R. Wu, *Phys. Rev. B* **97**, 115151 (2018).
- [11] A. J. Heinrich, J. A. Gupta, C. P. Lutz, and D. M. Eigler, *Science* **306**, 466 (2004).
- [12] A. A. Khajetoorians, S. Lounis, B. Chilian, A. T. Costa, L. Zhou, D. L. Mills, J. Wiebe, and R. Wiesendanger, *Phys. Rev. Lett.* **106**, 037205 (2011).
- [13] S. Murakami, *Phys. Rev. Lett.* **97**, 236805 (2006).
- [14] Z. Liu, C.-X. Liu, Y.-S. Wu, W.-H. Duan, F. Liu, and J. Wu, *Phys. Rev. Lett.* **107**, 136805 (2011).
- [15] I. K. Drozdov, A. Alexandradinata, S. Jeon, S. Nadj-Perge, H. Ji, R. J. Cava, B. Andrei Bernevig, and A. Yazdani, *Nature Physics* **10**, 664 (2014).
- [16] Z.-Q. Huang, F.-C. Chuang, C.-H. Hsu, Y.-T. Liu, H.-R. Chang, H. Lin, and A. Bansil, *Phys. Rev. B* **88**, 165301 (2013).
- [17] F. Yang, L. Miao, Z. F. Wang, M.-Y. Yao, F. Zhu, Y. R. Song, M.-X. Wang, J.-P. Xu, A. V. Fedorov, Z. Sun, G. B. Zhang, C. Liu, F. Liu, D. Qian, C. L. Gao, and J.-F. Jia, *Phys. Rev. Lett.* **109**, 016801 (2012).
- [18] T. Hirahara, G. Bihlmayer, Y. Sakamoto, M. Yamada, H. Miyazaki, S. Kimura, S. Blügel, and S. Hasegawa, *Phys. Rev. Lett.* **107**, 166801 (2011).
- [19] L. A. Agapito, A. Ferretti, A. Calzolari, S. Curtarolo, and M. Buongiorno Nardelli, *Phys. Rev. B* **88**, 165127 (2013).
- [20] L. A. Agapito, S. Curtarolo, and M. Buongiorno Nardelli, *Phys. Rev. X* **5**, 011006 (2015).
- [21] L. A. Agapito, M. Fornari, D. Ceresoli, A. Ferretti, S. Curtarolo, and M. B. Nardelli, *Phys. Rev. B* **93**, 125137 (2016).
- [22] L. A. Agapito, S. Ismail-Beigi, S. Curtarolo, M. Fornari, and M. B. Nardelli, *Phys. Rev. B* **93**, 035104 (2016).
- [23] M. B. Nardelli, F. T. Cerasoli, M. Costa, S. Curtarolo, R. D. Gennaro, M. Fornari, L. Liyanage, A. R. Supka, and H. Wang, *Computational Materials Science* **143**, 462 (2018).
- [24] Supplemental Material.
- [25] A. T. Costa, R. B. Muniz, S. Lounis, A. B. Klautau, and D. L. Mills, *Phys. Rev. B* **82**, 014428 (2010).
- [26] F. S. M. Guimarães, S. Lounis, A. T. Costa, and R. B. Muniz, *Phys. Rev. B* **92**, 220410 (2015).
- [27] J.-J. Zhu, D.-X. Yao, S.-C. Zhang, and K. Chang, *Phys. Rev. Lett.* **106**, 097201 (2011).
- [28] D. A. Abanin and D. A. Pesin, *Phys. Rev. Lett.* **106**, 136802 (2011).
- [29] In linear response theory the system is assumed to be arbitrarily close to equilibrium at all times. This means that the excitation energy is determined by the ground state electronic structure, and may differ from the MAE calculated via total energy differences.
- [30] A. T. Costa, R. B. Muniz, M. S. Ferreira, and D. L. Mills, *Phys. Rev. B* **78**, 214403 (2008).